Accepted Manuscript

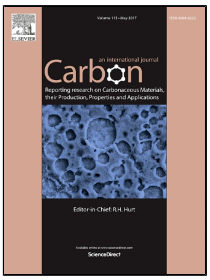

Twin graphene: A novel two-dimensional semiconducting carbon allotrope

Jin-Wu Jiang, Jiantao Leng, Jianxin Li, Zhengrong Guo, Tienchong Chang, Xingming Guo, Tongyi Zhang

PII:	S0008-6223(17)30308-1
DOI:	10.1016/j.carbon.2017.03.067
Reference:	CARBON 11874
To appear in:	*Carbon*
Received Date:	24 December 2016
Revised Date:	03 March 2017
Accepted Date:	20 March 2017

Please cite this article as: Jin-Wu Jiang, Jiantao Leng, Jianxin Li, Zhengrong Guo, Tienchong Chang, Xingming Guo, Tongyi Zhang, Twin graphene: A novel two-dimensional semiconducting carbon allotrope, *Carbon* (2017), doi: 10.1016/j.carbon.2017.03.067

Twin Graphene: A Novel Two-Dimensional Semiconducting Carbon Allotrope

Jin-Wu Jiang, Jiantao Leng, Jianxin Li, Zhengrong Guo, Tienchong Chang*, Xingming Guo, Tongyi Zhang

Shanghai Institute of Applied Mathematics and Mechanics, Shanghai Key Laboratory of Mechanics in Energy Engineering, Shanghai University, Shanghai 200072, People's Republic of China

Graphene has been expected to revolutionize the electronics, but suffered from its zero bandgap that will lead to an unacceptable leakage current in graphene-based transistors. Although a bandgap engineered graphene structure may have a bandgap, such bandgap is sensitively dependent on the geometry of the structure. Finding new two-dimensional (2D) semiconducting carbon allotropes is therefore extremely important for the new emerging all-carbon electronics. Based on first principles calculations, here we predict a new 2D semiconducting carbon allotrope, referred to as twin graphene. The allotrope has an intrinsic direct bandgap, very close to that of silicon and tunable by in-plane strain, indicating its great potential in nanoelectronics. The stability of twin graphene is carefully verified by both the first principles calculations and the molecular dynamics simulations. We determine also the mechanical properties of twin graphene, including the in-plane stiffness, Poisson's ratio, shear stiffness and bending stiffness. Its excellent electronic and mechanical properties suggest that twin graphene may have a significant impact on many disciplines and fields related to nanotechnology.

* Corresponding author. Tel: 86(21)56331208. Email: tchang@staff.shu.edu.cn.

1. Introduction

Carbon has amply demonstrated its ability to form a variety of allotropes [1-20]. Recent discoveries of low-dimensional synthetic carbon allotropes such as 0D C_{60} [3], quasi-1D nanotubes [4] and 2D graphene [7] have revolutionized many different scientific and technological areas and triggered enormous interest in inventing other carbon nanomaterials, sparking an era of synthetic carbon allotropes [21, 22]. In particular, graphene has been considered as a candidate material for future electronics applications because of its extremely high carrier mobility and excellent electrode-channel contact [23-25]. However, the intrinsic dispersion of graphene is gapless, which leads to an unacceptably high off-state current and a very low on/off ratio in graphene transistors. Although extensive efforts have been made to open a bandgap in different graphene nanostructures [26-34], the engineered bandgap is critically dependent on the configurations of these structures. Many other efforts have been devoted to the finding of other 2D semiconducting materials, e.g., MoS_2 monolayers [35-38] and phosphorus carbide [39], with a moderate bandgap that a high-performance transistor requires. Constructing all-carbon nanoelectronics remains a challenge for the community due to the lack of a 2D planar semiconducting carbon allotrope with an intrinsic moderate bandgap.

There have been quite few works proposing some 2D defect-based semiconducting carbon allotropes. For example, by introducing non-hexagonal polygon into sp^2 carbon networks, scientists have predicted possible 2D semiconductors including penta-graphene [15], H-net [40], Octite SC [33], BPC [41], etc. These semiconducting carbon structures have generated great interest in the field and offered the prospect of 2D circuit logic composed entirely of carbon.

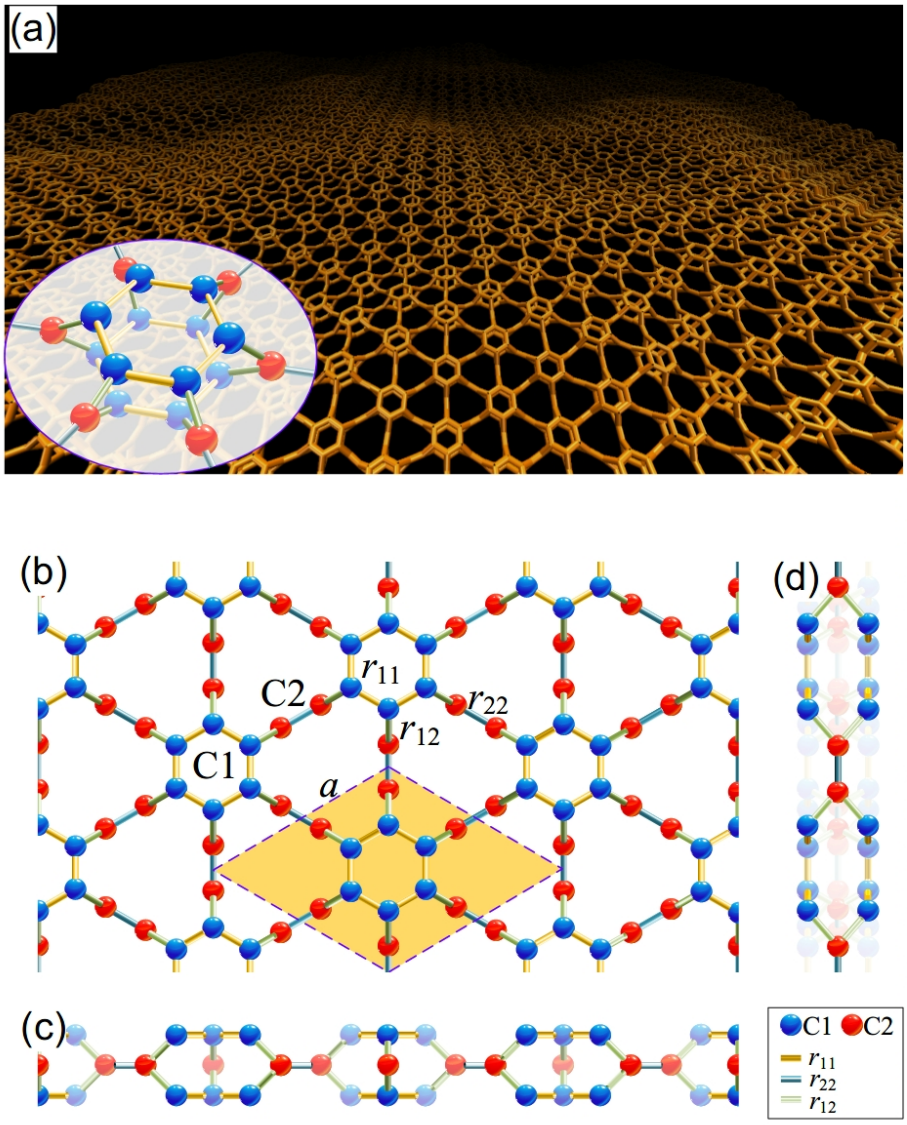

Figure 1. Structure of twin graphene. (a) Bird view of a twin graphene sheet. Shown in inset is the primitive unit cell C_{18}. (b)-(d) Top, front and right views of the lattice structure. The unit cell is marked by the dashed parallelogram. The two types of inequivalent carbon atoms are labeled C1 and C2, and the three types of carbon bonds are indicated by r_{11} (in yellow), r_{22} (in cyan), and r_{12} (in green).

In this paper, based on first principles calculations, we predict a novel 2D planar direct semiconducting carbon allotrope. The structure of the allotrope, shown in Figure 1, can be simply viewed as a result of replacing one-third of parallel aromatic bonds in AA-stacked bilayer graphene by carbon dimers. The allotrope is like a graphene bilayer in which one layer is organically conjoined with another, therefore we call it twin graphene. Our first principles calculations show that twin graphene is dynamically stable and is a direct semiconductor with an intrinsic bandgap of about 1 eV. This bandgap value is very close to that of silicon, one of the most important industrial semiconducting materials, making twin graphene a promising candidate for future nanoelectronics composed entirely of carbon.

2. Calculation methods

First principles (FP) calculations are performed using the SIESTA package [42]. The local density approximation (LDA) is applied to account for the exchange-correlation function with Ceperley-Alder parameterization [43] and the double-ζ (DZ) orbital basis set is adopted. For the geometry and basic electronic band structure, we have also used the generalized gradients approximation (GGA), with the exchange-correlation function parameterized by Perdew, Burke and Ernzerhof [44]. The double-ζ polarization (DZP) orbital basis set is also applied for the computation. During the conjugate-gradient optimization of twin graphene, the maximum force on each atom is required to be smaller than 0.005 eV/Å. A mesh cut off of 320 Ry is used. Periodic boundary condition is applied in the two in-plane directions. A vacuum space of 20.0 Å is introduced to sufficiently

separate the structure in the out-of-plane direction. The Monkhorst-Pack scheme is applied to sample the Brillouin zone with a mesh of 20×20×1 k-point sampling. For the computation of phonon dispersion, the force constant matrix is obtained by the finite differential approach, with a 5×5×1 supercell.

Molecular dynamics (MD) simulations are carried out using the LAMMPS package [45]. AIREBO potential [46] is used to describe the C-C bond interactions, where the vdW interactions between nonbonded atoms are described by a Lennard-Jones (L-J) 6-12 potential (with ε = 2.968 meV and σ = 0.3407 nm). A 200×200 Å twin graphene sheet is used to study its thermal conductivity and in-plane mechanical behavior. A series of twin graphene nanotube with different diameters are used to obtain the bending stiffness of twin graphene. The structure is optimized at 1 K. The structure optimization and in-plane mechanical property prediction are conducted under a NPT ensemble with in-plane periodic boundary conditions imposed, while the thermal stability is investigated under free boundary conditions. A Berendson thermostat is adopted to maintain both ends of the 200×200 Å sheet at 300 and 400 K to obtain the thermal conductivity at 350 K. To verify the thermal stability of twin graphene, MD simulations with both the AIREBO potential and the ReaxFF [47] (which can better model bond breaking and formation) for a 100×100 Å twin graphene sheet (within a calculation box of 200×200×100 Å) are performed under a NVT ensemble. A time step of 0.25 fs is used in all simulations.

3. Results and discussion

Twin graphene has a space group of P6/mmm in the Hermann-Mauguin notation, which is symmorphic and has the point group D_{6h}. There are two types of inequivalent carbon atoms in twin graphene, denoted C1 (on the surface planes) and C2 (on the mid-plane) respectively (Figure 1). A primitive unit cell contains 18 atoms (C_{18}), 12 of C1 and 6 of C2. The top-view configuration of twin graphene is similar to that of a one-atom-thick carbon allotrope, gamma-graphyne [48]. This means that twin graphene can also be viewed as a gamma-graphyne to which hexagonal carbon rings have been superimposed to the existing ones creating an all three-coordinated carbon structure. The optimized structural parameters for twin graphene from both first principles (FP) calculations and molecular dynamics (MD) simulations are summarized in Table I. The C1-C1 bond length, r_{11} = 1.42 Å, indicates the sp^2 hybridization of C1 atoms, whereas the C1–C2 (r_{12} = 1.55 Å) and C2–C2 (r_{22} = 1.34 Å) bond lengths exhibit featured characteristics of single and double bonds. We note that the smaller bond angle θ_{121} (or larger θ_{122}) from MD simulations is induced by the van der Waals interactions (particularly between C1 rings) which is not included in FP calculations.

Table I. Optimized lattice constant (a), bond lengths (r), bond angles (θ), and bandgap for twin graphene from different methods

Methods	a (Å)	r_{11} (Å)	r_{22} (Å)	r_{12} (Å)	θ_{111} (deg)	θ_{112} (deg)	θ_{121} (deg)	θ_{122} (deg)	bandgap (eV)
FP-LDA-DZ	6.11	1.42	1.34	1.53	120.0	108.5	101.2	129.4	0.981
FP-GGA-DZ	6.17	1.43	1.35	1.54	120.0	108.6	100.7	129.6	0.956

FP-LDA-DZP	6.08	1.41	1.34	1.52	120.0	108.4	101.8	129.1	0.760
FP-GGA-DZP	6.14	1.42	1.35	1.53	120.0	108.5	101.4	129.1	0.730
MD-AIREBO	6.43	1.43	1.33	1.55	120.0	112.4	80.6	139.7	-

The electric band structure and density of state (DOS) from FP-LDA-DZ calculations shown in Figure 2a for twin graphene indicate that this allotrope is a semiconductor with a direct bandgap of 0.981eV at the Γ point. We have compared the value of the bandgap obtained from different functionals (LDA and GGA) and different orbital basis sets (DZ and DZP) in Table I. We find that LDA and GGA give close value for the bandgap, while DZP leads to a smaller bandgap than DZ. In what follows, we discuss mainly the results from FP-LDA-DZ calculations except specified otherwise. The obtained bandgap value for twin graphene is close to that of silicon (1.17 eV), one of the most important industrial semiconducting materials, and a half of that of MoS2 monolayers (1.8~1.9 eV) [38, 49], one of the most promising 2D semiconducting materials. For comparison, the bandgap for diamond (that is an insulator) is about 4.16 eV, and the bandgap for T-carbon is 2.22 eV [9]. A bandgap engineered graphene-based nanostructure may open the bandgap of graphene. For example, graphene nanoribbons with homogeneous armchair or zigzag shaped edges [29, 31, 32], graphene with patterned defects [33, 50], stained graphene [28] and hydrogenated graphene [30], etc. all have bandgaps. However, the value of an engineered bandgap is critically dependent on the size, edge orientation, defect pattern and many other geometric parameters of the graphene structure [26-34]. Alternatively, twin graphene has an intrinsic bandgap, which provides a valuable supplement for the distribution of the electronic band gap of about 1.0 eV, and could therefore be a promising

candidate material for future electronics composed entirely of carbon [51]. In addition, considering its direct transition property, it is expected that this allotrope may gain wide applications in the field of electric optical devices working in the infra-red range.

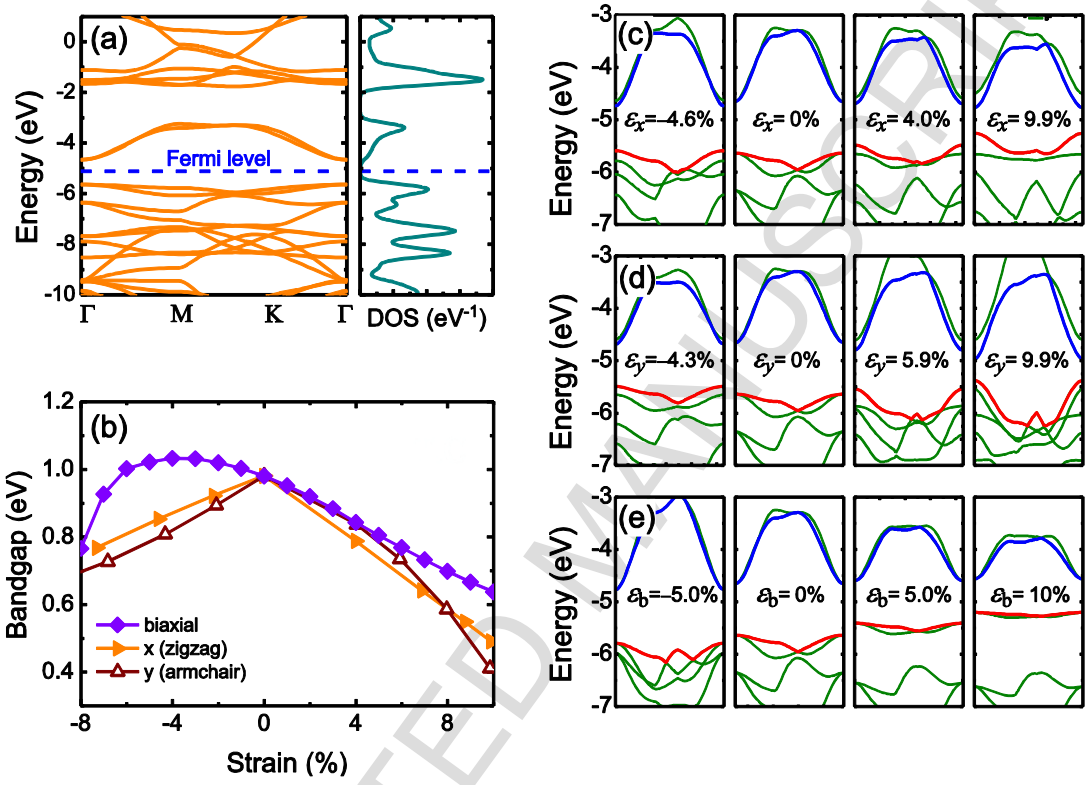

Figure 2. Electronic properties of twin graphene from FP-LDA-DZ calculations. (a) Electronic band structure and density of state (DOS) show that twin graphene is a direct semiconductor with an intrinsic bandgap of 0.981 eV at Γ point. (b) Twin graphene is a semiconductor in a large strain range. The band structures at different strains are shown in (c)-(e). The lowest conduction band and the highest valence band are displayed by the blue and red lines respectively. Three types of strains, i.e., zigzag-direction strain (ε_x), armchair-direction strain (ε_y), and biaxial strain (ε_b), are considered.

The electronic band structure of twin graphene can also be engineered by different types of mechanical strains, including the in-plane uniaxial strain and biaxial strain. As shown in Figure 2b, the bandgap of the twin graphene can be tuned by the mechanical strain in a wide range between 0.4 and 1.0 eV. The uniaxial tensile strain can shift the lowest conduction band downwards and the highest valence band upwards (see Figure 2c & 2d), whereas the biaxial tensile strain can efficiently modify the first two highest valence bands (see Figure 2e). It is quite interesting that, during a large strain range, the direct transition property of twin graphene is well kept, which maintains it to be a stable optical device with tunable frequency under mechanical strain.

To examine the dynamic stability of twin graphene, we show the calculated phonon dispersion properties in Figure 3a. It is important to see that there is no imaginary frequency in the full spectrum, which supports the mechanical stability of the predicted structure. The highest phonon frequency 1764 cm^{-1} for twin graphene is close to the highest phonon frequency of 1600 cm^{-1} for AA-stacked bilayer graphene, which reflects the bilayer-graphene-like structural bonding character of twin graphene. The acoustic velocities for the two in-plane branches are 2.38, and 4.05 km/s. We note that the lowest phonon branch corresponds to the out-of-plane vibration for twin graphene, which should be a flexural branch with quadratic dispersion. However, it is a linear dispersion in the present calculation, which is probably due to the finite cutoff for the long-range interaction. The in-plane acoustic velocities in twin graphene are smaller than those (above 10.0 km/s [52]) in graphene, indicating that the thermal conductivity in the new allotrope will be smaller than that of graphene. This is confirmed by our MD-AIREBO calculations which show that

the in-plane thermal conductivity of a 200×200 Å twin graphene sheet is 8.5 W $m^{-1}K^{-1}$ at 350 K, and those for the graphene and gamma-graphyne sheets with the same size are 95 and 125 W $m^{-1}K^{-1}$, respectively. MD simulations based on both the AIREBO potential and ReaxFF show that the inner region of a 100×100 Å twin graphene sheet can maintain its structural integrity within 250 ps at a high temperature up to 1800 K, which verifies the thermal stability of twin graphene, but may undergo a phase transition (the bond breaking always initiates at C1-C2 (r_{12}) bonds) at 2200 K. In particular, MD-ReaxFF simulations at 4000 K reveal that twin graphene will decompose into bilayer amorphous graphene phase (with a large number of defects and broken bonds, and a few interlayer bonds).

From an energetic point of view, a larger cohesive energy means better structural stability. As shown in Figure 3b, according to the results from the FP (based on both LDA and GGA approaches) and MD (based on AIREBO potential) calculations, the cohesive energy of twin graphene is (0.8-0.9 eV) smaller than that of graphene, approximately equal to (0.07-0.17 eV smaller than) that of gamma-graphyne (the most stable graphyne [53]), and (0.2-0.3 eV) larger than that of alpha-graphyne, indicating that twin graphene is nearly as stable as gamma-graphyne. Considering the successful synthesis of another theorized carbon allotrope, graphdiyne [54-56], which is theoretically predicted less stable than gamma-graphyne [10], we expect that it is possible to synthesize twin graphene in the near future.

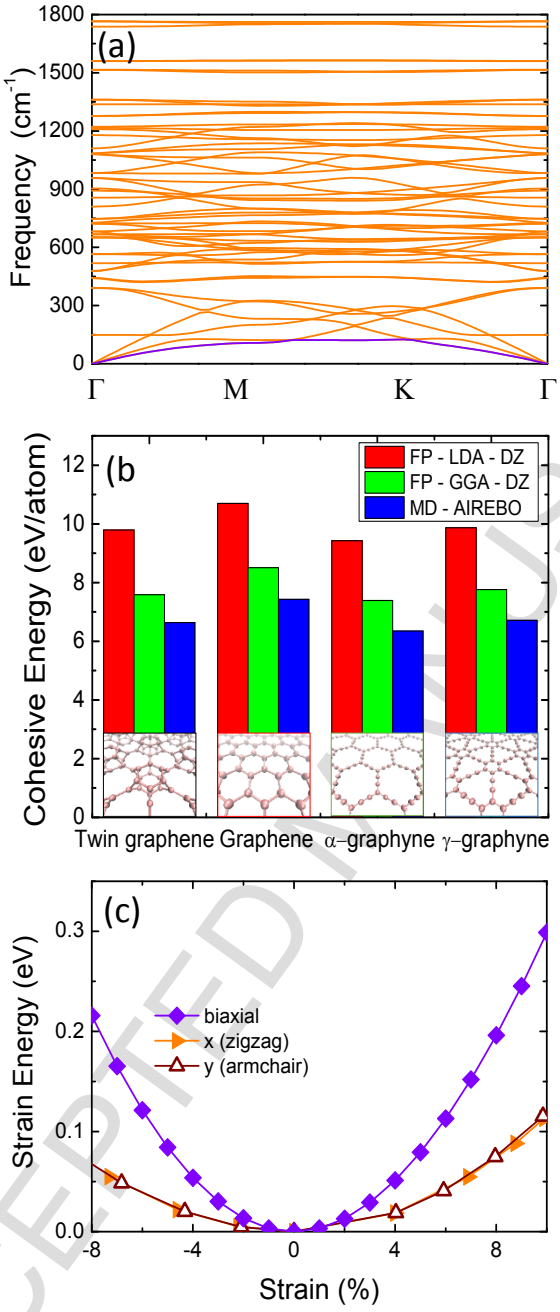

Figure 3. (a) Phonon spectrum of twin graphene. The highest frequency is close to that for AA-stacked bilayer graphene. The out-of-plane acoustic branch is colored blue. (b) Cohesive energy of twin graphene, with comparison with those of graphene, alpha-graphyne and gamma-graphyne. (c) Strain energy vs strain.

Elastic constants of a theorized material are not only important for its potential applications, but also can be used to test its mechanical stability. FP calculations of the strain energy per atom show that the strain energy responds almost identically to both in-plane direction strains (Figure 3c), which is indeed a result of its six-fold in-plane symmetry. A 2D isotropic material has two independent elastic constants that can be the in-plane stiffness and the Poisson's ratio, the in-plane stiffness and the shear stiffness, or the layer modulus and the shear stiffness. By fitting the strain energy to the parabolic function of the axial strain, we obtain an in-plane stiffness, Y_S, of about 186 N/m (20.9 eV/atom) for twin graphene, which is about a half of that for graphene (~360 N/m) and is slightly higher than that of gamma-graphyne (~150 N/m). The in-plane Poisson's ratio value from FP calculations is about 0.32. According to the isotropic elastic theory (which applies for six-fold symmetric materials), the in-plane shear stiffness of twin graphene, G_S, is calculated as $G_S = Y_S/[2(1+\nu)] = 70$ N/m, and the layer modulus $L = Y_S/[2(1-\nu)] = 137$ N/m. When twin graphene is treated as a 2D membrane, its elastic constants can be obtained as $C_{11} = Y_S/(1-\nu^2) = 207$ N/m, $C_{12} = \nu Y_S/(1-\nu^2) = 66$ N/m, and $C_{66} = G_S = 70$ N/m. These elastic constants satisfy $C_{11} > |C_{12}|$ and $C_{66} > 0$, further confirming the mechanical stability of twin graphene.

We study also the mechanical properties of twin graphene using MD-AIREBO simulations. Equivalent values to the results from FP calculations, 172 N/m (21.35 eV/atom) for the in-plane stiffness and 65 N/m for the shear stiffness, are obtained at 1 K, suggesting that the mechanical properties of twin graphene can be accurately predicted by MD-AIREBO calculations. Our simulations show also that the bending stiffness of twin graphene is about 1.39 eV, and the fracture strains at 300 K are about 17% and 16% in the

zigzag and armchair directions, respectively. These excellent mechanical properties, comparable to those of gamma-graphyne [57-61], can be considered a direct result of its all-carbon bonded structure.

Owing to its rich chemistry, carbon is one of the most important elements which can provide versatile opportunities for the construction of both natural and synthetic materials. However, despite many years of research, the detailed structure of many carbon materials remains poorly understood. For example, the measured X-ray diffraction (XRD) spectra indicate a high abundance of unknown carbon structures in detonation soot [62] and combustion fullerene soot [63]. To provide further information for the identification of twin graphene in experimental observation, we present the simulated XRD spectrum of AB-stacked twin graphene (periodic boundaries are imposed in three directions to model an infinite 3D structure) in Figure 4, in comparison with those of graphite, diamond and AB-stacked gamma-graphyne. The highest intensity peak appears at 15.8° for twin graphene, obviously distinct from those for other three carbon allotropes, and corresponds almost exactly to the peak around 16° of detonation soot [62] and combustion fullerene soot [63], suggesting that twin graphene is among the likely candidates for the unknown phases in soot.

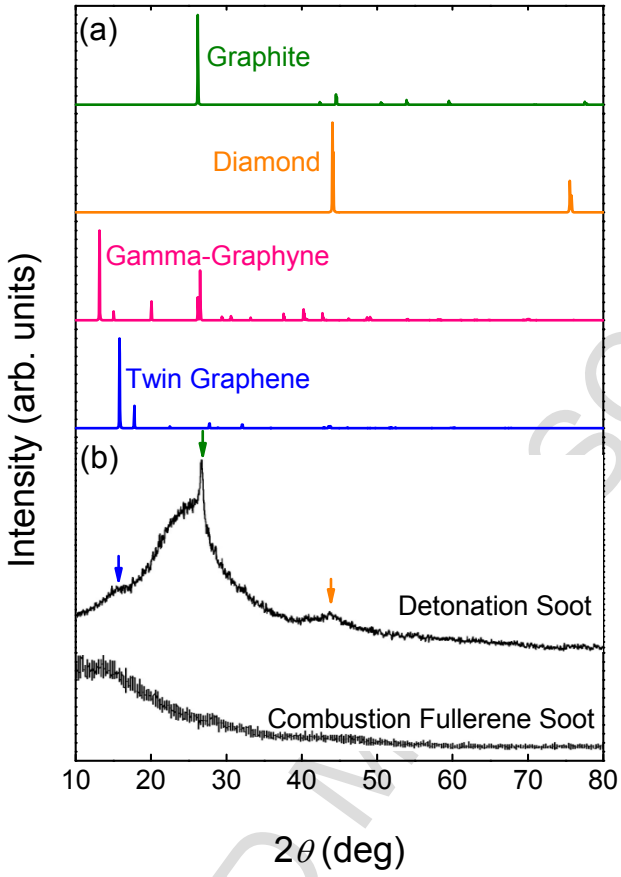

Figure 4. (a) The simulated X-Ray diffraction patterns for graphite, diamond, gamma-graphyne, and twin graphene. (b) Experimental X-Ray diffraction patterns for detonation soot [62] of pure TNT and combustion fullerene soot [63]. Arrows indicate the intensity peaks corresponding to the highest ones for twin graphene, graphite and diamond. X-ray wavelength is 1.5406 Å with a copper source.

4. Conclusion

In conclusion, we have predicted a new phase of 2D semiconducting carbon allotrope, twin graphene. Its stability is carefully verified using both the first principles calculations and the molecular dynamics simulations. The cohesive energy of twin graphene is close to that of gamma-graphyne. The intrinsic moderate bandgap, 2D planar shape, as well as all-carbon structure of twin graphene allow it to serve as a semiconductor candidate in the future all-carbon electronics. The excellent mechanical properties make twin graphene suitable to be used in nanoelectromechanical systems. In addition, similar to graphene, twin graphene has potential to be rolled up to form twin-graphene nanotubes or to be stacked to form 3D graphite-like structures, which may not only attract broad interest from the nanotechnology community but also may have significant impacts on many other disciplines.

Acknowledgements

This work is supported by NSFC (Grant Nos. 11425209, 11504225), the Recruitment Program of Global Youth Experts of China, and the Shanghai Pujiang Program (Grant No. 13PJD016). The MD simulations were carried out on the computing platform of the International Center for Applied Mechanics in Energy Engineering (ICAMEE), Shanghai University.

References

[1] Liu M, Artyukhov VI, Lee H, Xu F, Yakobson BI. Carbyne from First Principles: Chain of C Atoms, a Nanorod or a Nanorope. ACS Nano. 2013;7(11):10075-82.

[2] Hoffmann R, Hughbanks T, Kertesz M, Bird PH. Hypothetical metallic allotrope of carbon. Journal of the American Chemical Society. 1983;105(14):4831-2.

[3] Kroto HW, Heath JR, O'Brien SC, Curl RF, Smalley RE. C60: Buckminsterfullerene. Nature. 1985;318(6042):162-3.

[4] Iijima S. Helical microtubules of graphitic carbon. Nature. 1991;354(6348):56-8.

[5] Liu AY, Cohen ML. Theoretical study of a hypothetical metallic phase of carbon. Physical Review B. 1992;45(9):4579-81.

[6] O'Keeffe M, Adams GB, Sankey OF. Predicted new low energy forms of carbon. Physical Review Letters. 1992;68(15):2325-8.

[7] Novoselov KS, Geim AK, Morozov SV, Jiang D, Zhang Y, Dubonos SV, et al. Electric Field Effect in Atomically Thin Carbon Films. Science. 2004;306(5696):666-9.

[8] Zhu L, Wang J, Zhang T, Ma L, Lim CW, Ding F, et al. Mechanically Robust Tri-Wing Graphene Nanoribbons with Tunable Electronic and Magnetic Properties. Nano Letters. 2010;10(2):494-8.

[9] Sheng X-L, Yan Q-B, Ye F, Zheng Q-R, Su G. T-Carbon: A Novel Carbon Allotrope. Physical Review Letters. 2011;106(15):155703.

[10] Sheng X-L, Cui H-J, Ye F, Yan Q-B, Zheng Q-R, Su G. Octagraphene as a versatile carbon atomic sheet for novel nanotubes, unconventional fullerenes, and hydrogen storage. Journal of Applied Physics. 2012;112(7):074315.

[11] Chen Y, Xie Y, Yang SA, Pan H, Zhang F, Cohen ML, et al. Nanostructured Carbon Allotropes with Weyl-like Loops and Points. Nano Letters. 2015;15(10):6974-8.

[12] Roman RE, Kwan K, Cranford SW. Mechanical Properties and Defect Sensitivity of Diamond Nanothreads. Nano Letters. 2015;15(3):1585-90.

[13] Wang Z, Zhou X-F, Zhang X, Zhu Q, Dong H, Zhao M, et al. Phagraphene: A Low-Energy Graphene Allotrope Composed of 5–6–7 Carbon Rings with Distorted Dirac Cones. Nano Letters. 2015;15(9):6182-6.

[14] Xu E-s, Lammert PE, Crespi VH. Systematic Enumeration of sp3 Nanothreads. Nano Letters. 2015;15(8):5124-30.

[15] Zhang S, Zhou J, Wang Q, Chen X, Kawazoe Y, Jena P. Penta-graphene: A new carbon allotrope. Proceedings of the National Academy of Sciences. 2015;112(8):2372-7.

[16] Wang J-T, Weng H, Nie S, Fang Z, Kawazoe Y, Chen C. Body-Centered Orthorhombic C16: A Novel Topological Node-Line Semimetal. Physical Review Letters. 2016;116(19):195501.

[17] Wang Z, Dong F, Shen B, Zhang RJ, Zheng YX, Chen LY, et al. Electronic and optical properties of novel carbon allotropes. Carbon. 2016;101:77-85.

[18] Zhang X, Wei L, Tan J, Zhao M. Prediction of an ultrasoft graphene allotrope with Dirac cones. Carbon. 2016;105:323-9.

[19] He C, Zhang CX, Xiao H, Meng L, Zhong JX. New candidate for the simple cubic carbon sample shock-synthesized by compression of the mixture of carbon black and tetracyanoethylene. Carbon. 2017;112:91-6.

[20] Li Z, Hu M, Ma M, Gao Y, Xu B, He J, et al. Superhard superstrong carbon clathrate. Carbon. 2016;105:151-5.

[21] Hirsch A. The era of carbon allotropes. Nat Mater. 2010;9(11):868-71.

[22] Georgakilas V, Perman JA, Tucek J, Zboril R. Broad Family of Carbon Nanoallotropes: Classification, Chemistry, and Applications of Fullerenes, Carbon Dots, Nanotubes, Graphene, Nanodiamonds, and Combined Superstructures. Chemical Reviews. 2015;115(11):4744-822.

[23] Schwierz F. Graphene transistors. Nat Nano. 2010;5(7):487-96.

[24] Geim AK, Novoselov KS. The rise of graphene. Nat Mater. 2007;6(3):183-91.

[25] Sun J, Zheng G, Lee H-W, Liu N, Wang H, Yao H, et al. Formation of Stable Phosphorus–Carbon Bond for Enhanced Performance in Black Phosphorus Nanoparticle–Graphite Composite Battery Anodes. Nano Letters. 2014;14(8):4573-80.

[26] Novoselov K. Graphene: Mind the gap. Nat Mater. 2007;6(10):720-1.

[27] Chen Y-C, Cao T, Chen C, Pedramrazi Z, Haberer D, de OteyzaDimas G, et al. Molecular bandgap engineering of bottom-up synthesized graphene nanoribbon heterojunctions. Nat Nano. 2015;10(2):156-60.

[28] Gui G, Li J, Zhong J. Band structure engineering of graphene by strain: First-principles calculations. Physical Review B. 2008;78(7):075435.

[29] Han MY, Özyilmaz B, Zhang Y, Kim P. Energy Band-Gap Engineering of Graphene Nanoribbons. Physical Review Letters. 2007;98(20):206805.

[30] Balog R, Jorgensen B, Nilsson L, Andersen M, Rienks E, Bianchi M, et al. Bandgap opening in graphene induced by patterned hydrogen adsorption. Nat Mater. 2010;9(4):315-9.

[31] Son Y-W, Cohen ML, Louie SG. Energy Gaps in Graphene Nanoribbons. Physical Review Letters. 2006;97(21):216803.

[32] Barone V, Hod O, Scuseria GE. Electronic Structure and Stability of Semiconducting Graphene Nanoribbons. Nano Letters. 2006;6(12):2748-54.

[33] Appelhans DJ, Lin Z, Lusk MT. Two-dimensional carbon semiconductor: Density functional theory calculations. Physical Review B. 2010;82(7):073410.

[34] Bischoff D, Varlet A, Simonet P, Eich M, Overweg HC, Ihn T, et al. Localized charge carriers in graphene nanodevices. Applied Physics Reviews. 2015;2(3):031301.

[35] Qiao J, Kong X, Hu Z-X, Yang F, Ji W. High-mobility transport anisotropy and linear dichroism in few-layer black phosphorus. Nature Communications. 2014;5:4475.

[36] Desai SB, Madhvapathy SR, Sachid AB, Llinas JP, Wang Q, Ahn GH, et al. MoS2 transistors with 1-nanometer gate lengths. Science. 2016;354(6308):99-102.

[37] Radisavljevic B, Radenovic A, Brivio J, Giacometti V, Kis A. Single-layer MoS2 transistors. Nat Nano. 2011;6(3):147-50.

[38] Mak KF, Lee C, Hone J, Shan J, Heinz TF. Atomically Thin ${\mathrm{MoS}}_{2}$: A New Direct-Gap Semiconductor. Physical Review Letters. 2010;105(13):136805.

[39] Guan J, Liu D, Zhu Z, Tománek D. Two-Dimensional Phosphorus Carbide: Competition between sp2 and sp3 Bonding. Nano Letters. 2016;16(5):3247-52.

[40] Hu M, Shu Y, Cui L, Xu B, Yu D, He J. Theoretical two-atom thick semiconducting carbon sheet. Physical Chemistry Chemical Physics. 2014;16(34):18118-23.

[41] Brunetto G, Autreto PAS, Machado LD, Santos BI, dos Santos RPB, Galvão DS. Nonzero Gap Two-Dimensional Carbon Allotrope from Porous Graphene. The Journal of Physical Chemistry C. 2012;116(23):12810-3.

[42] José MS, Emilio A, Julian DG, Alberto G, Javier J, Pablo O, et al. The SIESTA method for ab initio order- N materials simulation. Journal of Physics: Condensed Matter. 2002;14(11):2745.

[43] Ceperley DM, Alder BJ. Ground State of the Electron Gas by a Stochastic Method. Physical Review Letters. 1980;45(7):566-9.

[44] Perdew JP, Burke K, Ernzerhof M. Generalized Gradient Approximation Made Simple. Physical Review Letters. 1996;77(18):3865-8.

[45] Plimpton S. Fast parallel algorithms for short-range molecular dynamics. Journal of Computational Physics. 1995;117(1):1-19.

[46] Brenner D, Shenderova O, Harrison J. SJ Stuart, B. Ni, SB Sinnott. J Phys: Condens Matter. 2002;14(783):7.

[47] van Duin ACT, Dasgupta S, Lorant F, Goddard WA. ReaxFF: A Reactive Force Field for Hydrocarbons. The Journal of Physical Chemistry A. 2001;105(41):9396-409.

[48] Baughman RH, Eckhardt H, Kertesz M. Structure‐property predictions for new planar forms of carbon: Layered phases containing sp2 and sp atoms. The Journal of Chemical Physics. 1987;87(11):6687-99.

[49] Li T, Galli G. Electronic Properties of MoS2 Nanoparticles. The Journal of Physical Chemistry C. 2007;111(44):16192-6.

[50] Su C, Jiang H, Feng J. Two-dimensional carbon allotrope with strong electronic anisotropy. Physical Review B. 2013;87(7):075453.

[51] Zhang Y-Y, Chen S, Xiang H, Gong X-G. Hybrid crystalline sp2-sp3 carbon as a high-efficiency solar cell absorber. Carbon. 2016;109:246-52.

[52] Jiang J-W, Tang H, Wang B-S, Su Z-B. Chiral symmetry analysis and rigid rotational invariance for the lattice dynamics of single-wall carbon nanotubes. Physical Review B. 2006;73(23):235434.

[53] Kim H, Kim Y, Kim J, Kim WY. Computational searching for new stable graphyne structures and their electronic properties. Carbon. 2016;98:404-10.

[54] Li G, Li Y, Liu H, Guo Y, Li Y, Zhu D. Architecture of graphdiyne nanoscale films. Chemical Communications. 2010;46(19):3256-8.

[55] Zhou J, Gao X, Liu R, Xie Z, Yang J, Zhang S, et al. Synthesis of Graphdiyne Nanowalls Using Acetylenic Coupling Reaction. Journal of the American Chemical Society. 2015;137(24):7596-9.

[56] Gao X, Li J, Du R, Zhou J, Huang M-Y, Liu R, et al. Direct Synthesis of Graphdiyne Nanowalls on Arbitrary Substrates and Its Application for Photoelectrochemical Water Splitting Cell. Advanced Materials. 2016:1605308.

[57] Cranford SW, Buehler MJ. Mechanical properties of graphyne. Carbon. 2011;49(13):4111-21.

[58] Wang S, Fan Z, Cui Y, Zhang S, Yang B, Chen H. Fracture behaviors of brittle and ductile 2D carbon structures under uniaxial tensile stress. Carbon. 2017;111:486-92.

[59] Sun H, Mukherjee S, Daly M, Krishnan A, Karigerasi MH, Singh CV. New insights into the structure-nonlinear mechanical property relations for graphene allotropes. Carbon. 2016;110:443-57.

[60] Puigdollers AR, Alonso G, Gamallo P. First-principles study of structural, elastic and electronic properties of α-, β- and γ-graphyne. Carbon. 2016;96:879-87.

[61] Hou J, Yin Z, Zhang Y, Chang T. An Analytical Molecular Mechanics Model for Elastic Properties of Graphyne-n. Journal of Applied Mechanics. 2015;82(9):094501--5.

[62] Chen P, Huang F, Yun S. Characterization of the condensed carbon in detonation soot. Carbon. 2003;41(11):2093-9.

[63] Zhu W, Miser DE, Geoffrey Chan W, Hajaligol MR. Characterization of combustion fullerene soot, C60, and mixed fullerene. Carbon. 2004;42(8–9):1463-71.

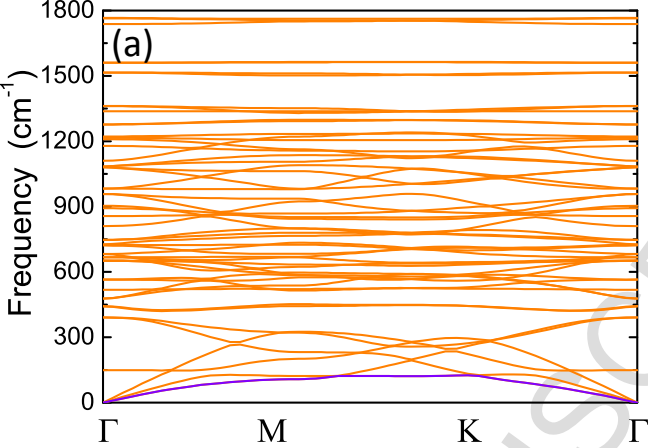
(a)
Frequency (cm-1)
1800
1500
1200
900
600
300
0
Γ
M
K
Γ

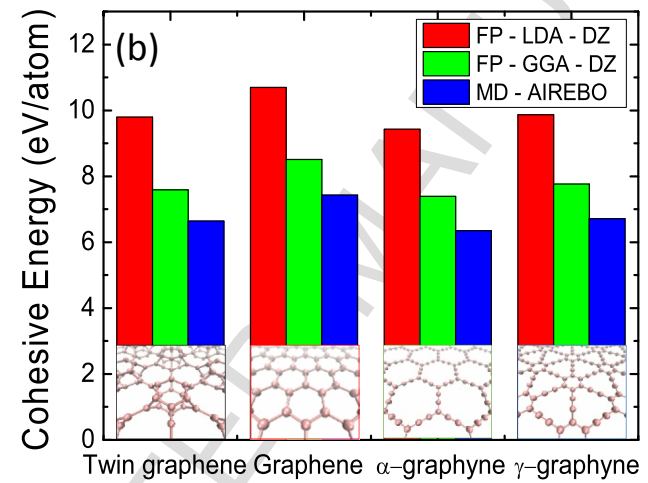
(b)
FP - LDA - DZ
FP - GGA - DZ
MD - AIREBO
Cohesive Energy (eV/atom)
12
10
8
6
4
2
0
Twin graphene
Graphene
α–graphyne
γ–graphyne

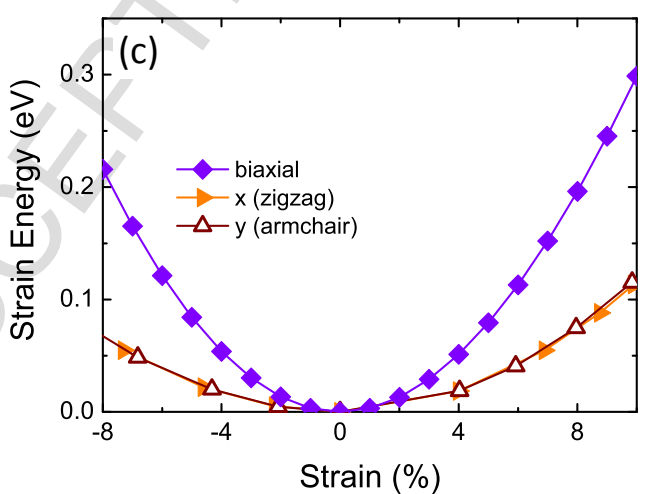
(c)
biaxial
x (zigzag)
y (armchair)
Strain Energy (eV)
0.3
0.2
0.1
0.0
-8
-4
0
4
8
Strain (%)

Graphical Abstract

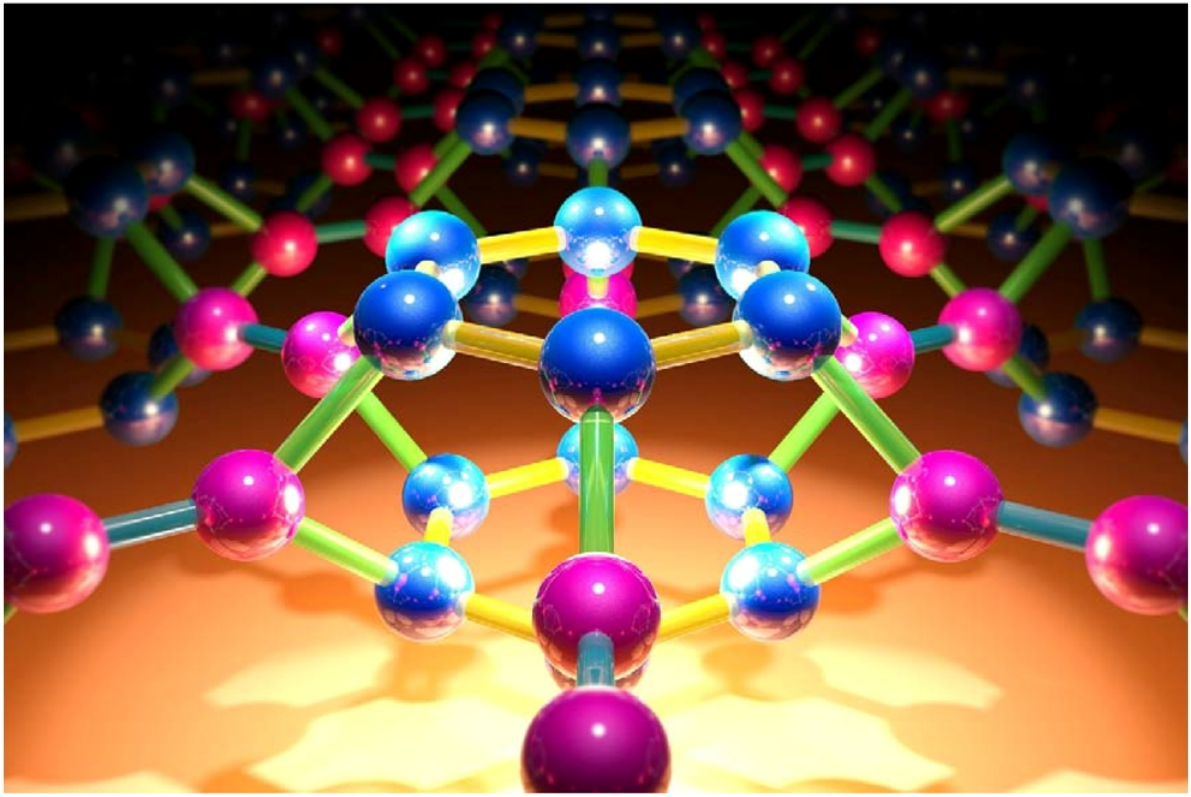

First principles calculations predict a new phase of two-dimensional planar semiconducting allotrope with an intrinsic bandgap which may overcome the main drawback of graphene for electronics applications.